Photochemical & Photobiological Sciences

PAPER

View Article Online
View Journal | View Issue

Cite this: *Photochem. Photobiol. Sci.*, 2018, **17**, 1068

Terpyridine derivatives as "turn-on" fluorescence chemosensors for the selective and sensitive detection of Zn^{2+} ions in solution and in live cells†

Tripti Mandal,[a] Anowar Hossain,[a] Anamika Dhara,[a] Abdulla Al Masum,[b] Saugata Konar,[c] Saikat Kumar Manna,*[d] Saikat Kumar Seth,[e] Sudipta Pathak*[d] and Subrata Mukhopadhyay[a]

Received 1st May 2018,
Accepted 6th June 2018

DOI: 10.1039/c8pp00186c

rsc.li/pps

A terpyridine based compound **L1** was designed and synthesized as an "off–on" chemosensor for the detection of Zn^{2+}. Chemosensor **L1** showed excellent selectivity and sensitivity toward Zn^{2+} by exhibiting a large fluorescence enhancement (~51-fold) at 370 nm whereas other competitive metal ions did not show any noticeable change in the emission spectra of chemosensor **L1**. The chemosensor (**L1**) was shown to detect Zn^{2+} ions down to 9.76 μM at pH 7.4. However, chemosensor **L1** binds Zn^{2+} in a 1 : 2 ratio (receptor : metal) with an association constant of 1.85×10^4 (R^2 = 0.993) and this 1 : 2 stoichiometric fashion is established on the basis of a Job plot and mass spectroscopy. DFT/TD-DFT calculations were carried out to understand the binding nature, coordination features and electronic properties of **L1** and the **L1**–$2Zn^{2+}$ complex. In addition, this "turn-on" fluorescence probe was effectively used to image intracellular Zn^{2+} ions in cultured MDA-MB-468 cells.

Introduction

One of the contemporary thrust areas where the scientific community finds great interest is the detection and determination of transition metal ions at low concentration levels due to their biological, analytical, medicinal and environmental importance.[1,2] Among these metal ions, the Zn^{2+} ion is one of the most abundant d-block transition metals and an essential trace element in the human body with the average human body containing 2–3 g of Zn^{2+} and a Zn^{2+} concentration as high as 10 μM in serum.[3,4] Zn^{2+} plays a vital role in many necessary physiological processes such as enzyme regulation, brain function, protein synthesis, neurotransmission, regulation of metalloenzymes, cellular apoptosis, DNA repair, gene expression and mammalian reproduction.[5–7] In spite of its essential role in living organisms, anomalous zinc metabolism is associated with a variety of severe neurological diseases such as Alzheimer's, Parkinson's, and Wilson's diseases, amyotrophic lateral sclerosis (ALS), ischemia and epilepsy.[8,9] Moreover, zinc is a food waste and an agricultural product in the environment; considerable concentrations of which have phytotoxic effects on soil microbes.[10] Therefore, recognizing the above physiological importance of zinc and its biomedical significance, there is growing interest in developing a noninvasive and sensitive method to trace and visually detect free zinc ions. As the zinc ion itself is magnetically and spectroscopically silent because of its $3d^{10}4S^0$ electron configuration, the development of simple, rapid, proficient, highly sensitive and selective zinc fluorescent chemosensors is of high importance not only for the elemental research but also for biological applications in living cells.[11] To date, several fluorescent and colorimetric chemosensors for zinc ions have been designed and reported.[12,13] However, it is still an enormous challenge to develop fluorescent chemosensors that can selectively detect Zn^{2+} ions without any interference of other transition metal ions, mainly Cd^{2+}, because both Zn^{2+} and Cd^{2+} are in the same group of the periodic table and have comparable properties. Consequently, they often induce similar spectroscopic changes on interaction with fluorescent chemosensors.[14] Besides, most of the reported zinc sensors are synthesized following multistep processes which are quite time consuming and not economical (Table S3†).[15] Thus, there is an immense need for the development of sensitive and selective Zn^{2+} sensors that can be prepared easily and economically.

[a]*Department of Chemistry, Jadavpur University, Kolkata 700032, India*
[b]*Department of Life Science & Bio-technology, Jadavpur University, Kolkata 700032, India*
[c]*Department of Chemistry, The Bhawanipur Education Society College, Kolkata 700 020, India*
[d]*Department of Chemistry, Haldia Government College, Debhog, Purba Medinipur, West Bengal 721657, India. E-mail: sudiptachemster@gmail.com, saikat.manna.chem@gmail.com*
[e]*Department of Physics, Jadavpur University, Kolkata 700032, India*
†Electronic supplementary information (ESI) available. See DOI: 10.1039/c8pp00186c

2,2′:6′,2″-Terpyridine and its derivatives represent a significant class of ligands in the areas of supramolecular chemistry, materials science and coordination chemistry[16] due to their strong binding ability towards various transition metal ions with their appropriately arranged ring nitrogens. Such strong chelating properties of terpyridine make them more useful building blocks for various technological applications such as in organic light-emitting devices and probes, dye sensitized solar cells, and mixed-valence chemistry as well as in two-photon luminescence systems and electrochromic devices.[17]

With all the abovementioned criteria in mind, herein we report three terpyridine based fluorescent 'off–on' probes, 4′,4‴′-(1,4-phenylene)bis(2,2′:6′,2″-terpyridine) (**L1**); 4′,4‴′-(1,3-phenylene)bis-2,2′:6′,2″-terpyridine (**L2**) and 2,4,6-tris(2-pyridyl)-*s*-triazine (**L3**) which can selectively detect Zn^{2+} ions in semi-aqueous solutions. Among them, **L1** was found to have the most potential as a turn-on fluorescence probe for Zn^{2+}. To determine the binding nature and coordination features of the complex (**L1**–2Zn^{2+}), we performed DFT computational studies using Gaussian software. Moreover, we have conducted fluorescence based bio-imaging experiments in MDA-MB-468 cells using **L1**.

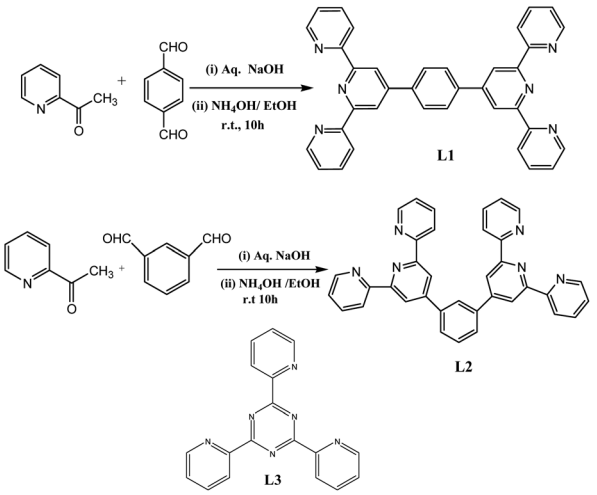

Scheme 1 Synthetic route for chemosensors **L1** and **L2** and the structure of chemosensor **L3**.

Experimental

Instrumentation and materials

^{1}H NMR spectra were recorded on a Bruker 300 MHz instrument. For NMR spectra, $CDCl_3$ was used as a solvent with TMS as an internal standard. Chemical shifts are expressed in ppm (δ) units. Mass spectra were recorded using a HRMS QTOF Micro YA263 mass spectrometer. UV-visible and fluorescence spectra measurements were performed on a JASCO V530 and a PerkinElmer LS-55 spectrofluorimeter, respectively. Chemicals used for the synthesis of **L1** and **L2** were purchased from Sigma Aldrich Chemical Co. (USA) and used without further purification. Fluorescent probe **L3** is commercially available from Sigma Aldrich Chemical Co. (USA) (Scheme 1). Salts of different cations and solvents were purchased from a commercial supplier, stored in desiccators under vacuum containing self-indicating silica, and used without any further purification. The following abbreviations are used to describe spin multiplicities in ^{1}H NMR spectra: s = singlet; d = doublet; t = triplet; and m = multiplet.

General method of UV-Vis and fluorescence spectral studies

For UV-vis and fluorescence titrations, stock solutions of sensors **L1**, **L2** and **L3** (4×10^{-5} M) were prepared in CH_3CN/H_2O (9 : 1, v/v, 10 mM HEPES buffer, pH 7.4) solution. Solutions of 4×10^{-4} M salts of the respective cations were prepared in Millipore water. In titration experiments, solutions of each chemosensor (4×10^{-5} M) were filled each time in a quartz optical cell of 1.00 cm optical path length, and the metal ion stock solutions were added into the quartz optical cell gradually by using a micropipette. Spectral data were recorded 1 min after the addition of the ions.

Preparation of 4′,4‴′-(1,4-phenylene)bis(2,2′:6′,2″-terpyridine) [L1]

Acetylpyridine (3.65 g, 30 mmol, 4 equivalents) was added to the ethanolic solution (100 mL) of terephthalaldehyde (1.0 g, 7.5 mmol, 1 equivalent). 10 mL of 1 molar aqueous solution of NaOH was poured into the reaction mixture at 25 °C, followed by 40 mL aqueous NH_3 (35%) solution. The reaction mixture was then stirred at 25 °C for 10 hours. A yellow solid was formed which was collected by filtration and washed with ethanol several times and dried in air. The desired product was obtained as a yellow solid. Unlike the reported literature, this reaction was carried out in a single step with satisfactory yield and acceptable purity. Yellow solid (2.51 g, 62%); M.P. >300 °C; IR (KBr): (cm^{-1}) 1667, 1602, 1566; ^{1}H NMR (300 MHz, $CDCl_3$) δ in ppm: 8.80 (s, 4H), 8.76 (d, J = 3.76 Hz, 4H), 8.69 (d, J = 7.0 Hz, 4H), 8.06 (s, 4H), 7.90 (t, J = 7.1 Hz, 4H), 7.37 (t, J = 4.2 Hz, 4H); anal. calcd for $C_{36}H_{24}N_6$: C, 79.98; H, 4.47; N, 15.55. Found C, 79.87; H, 4.42; N, 15.64; ES + TOF MS: m/z 541.1332 $[M + H]^+$ (calc. for $C_{36}H_{25}N_6^+$ 541.2136), 271.0494 $[M + 2H]^{2+}$ (calc. for $C_{28}H_{26}N_6^{2+}$ 271.1104).

Preparation of (4′,4‴′-(1,3-phenylene)bis-2,2′:6′,2″-terpyridine) (L2)

Acetylpyridine (3.65 g, 30 mmol, 4 equivalents) was added to the ethanolic solution (100 mL) of isophthalaldehyde (1.0 g, 7.5 mmol, 1 equivalent) at 25 °C. 10 mL of 1 molar aqueous solution of NaOH followed by 40 mL aqueous NH_3 (35%) solution was poured into the reaction mixture. The reaction mixture was then stirred for 10 hours. After that, a yellowish solid was formed which was collected by filtration and washed with ethanol several times and dried in air. Yellow solid (2.37 g, 58%); M.P. >300 °C; IR (KBr): (cm^{-1}) 1673, 1601, 1584, 1567; ^{1}H NMR (300 MHz, $CDCl_3$) δ in ppm: 8.84–8.38 (m, 8H), 8.38–8.02 (m, 2H), 7.99–7.66 (m, 8H), 7.55–7.25 (m, 5H), 7.00–6.89 (m, 1H); anal. calcd for $C_{36}H_{24}N_6$: C, 79.98; H, 4.47;

N, 15.55. Found C, 79.83; H, 4.51; N, 15.67; ES + TOF MS: *m*/*z* 541.1523 $[M + H]^+$ (calc. for $C_{36}H_{25}N_6^+$ 541.2136).

Computational studies

All geometries for **L1** and **L1**–2Zn^{2+} were optimized by density functional theory (DFT) calculations using the Gaussian09 (B3LYP/6-311G(d,p)) software package.[18]

Calculations for detection limit

The detection limit (DL) of **L1** for Zn^{2+} was determined using the following equation:[19]

$$DL = K \times Sb1/S,$$

where K = 2 or 3 (we take 2 in this case); $Sb1$ is the standard deviation of the blank solution; and S is the slope of the calibration curve.

Binding constant calculation using fluorescence titration data

The association constant and stoichiometry for the formation of the respective complexes were evaluated using the Benesi–Hildebrand (B–H) plot (eqn (1)):[20]

$$1/(I - I_0) = 1/K(I_{max} - I_0)[M^{n+}] + 1/(I_{max} - I_0) \quad (1)$$

where I_0, I_{max}, and I represent the emission intensity of free **L1**, the maximum emission intensity observed in the presence of the added metal ion at 370 nm for Zn^{2+} (λ_{ext} = 312 nm), and the emission intensity at a certain concentration of the metal ion added, respectively.

Cell imaging experiments

Minimum inhibitory concentration (MIC). A test tube containing LB broth was taken and a single colony of the organism was inoculated. The tube was incubated at 37 °C overnight. The following day two test tubes each containing LB broth were taken. 50 μl of the overnight grown culture was inoculated in both test tubes and incubated at 37 °C for 3–4 h. OD at 600 nm was measured for each of these tubes and recorded as the control for future reference. After that, different dilutions of the probe **L1** were prepared (*i.e.* stock, half dilution and one-fourth dilution). Next, 50 μl of the probe **L1** with different dilutions was added into each of the tubes, respectively. These tubes were incubated at 37 °C overnight. Another set of test tubes containing only the broth and probe **L** were incubated overnight. OD at 600 nm was measured for each of these tubes.

Cell survivability assay

The inhibition of cell growth was measured by MTT assay. In brief, cells were seeded in 96 well plates at 1 × 10^4 cells per well and exposed to probe **L1** at different concentrations for 24 h. After incubation, the cells were washed twice with 1× PBS and incubated with MTT solution (450 μg ml^{-1}) for 3–4 h at 37 °C. The resulting formazan crystals were dissolved in a MTT solubilization buffer and the absorbance was measured at 570 nm by using a microplate reader (Biotek, USA). Each point was assessed in triplicate.

Cell imaging

For confocal imaging studies, 1 × 10^4 MDA-MB-468 cells in 1000 μL of medium were seeded in a sterile 35 mm glass bottom culture dish (ibidi GmbH, Germany), and incubated at 37 °C in a CO_2 incubator for 10 hours. Then, the cells were washed with 500 μL DMEM followed by incubation with probe **L1** (10 μM) dissolved in 500 μL DMEM at 37 °C for 30 minutes in a CO_2 incubator and observed under an Olympus IX81 microscope equipped with a FV1000 confocal system using 1003 oil immersion Plan Apo (N.A. 1.45) objectives. Images obtained through section scanning were analyzed using Olympus Fluoview (version 3.1a; Tokyo, Japan) with excitation by a 350 nm monochromatic laser beam, and emission spectra were integrated over the range of 470 nm (single channel).

Results and discussion

Synthesis

The chemosensor molecules **L1** and **L2** were synthesized following a modified literature method[21] as shown in Scheme 1.

UV-vis and fluorescence studies

The sensing behaviour of compound **L1** toward different metal cations such as Li^+, K^+, Na^+, Mg^{2+}, Ca^{2+}, Sr^{2+}, Ba^{2+}, Mn^{2+}, Fe^{2+}, Co^{2+}, Ni^{2+}, Cu^{2+}, Cd^{2+}, Pb^{2+}, Hg^{2+}, Pd^{2+}, Al^{3+}, and Ag^+ and its superior selectivity toward Zn^{2+} over the other ions were investigated by UV-vis and fluorescence spectroscopy. All the spectroscopic studies were carried out in CH_3CN/H_2O (9 : 1, v/v, 10 mM HEPES buffer, pH 7.4) solution by adding aliquots of different metal cations dissolved in water.

The UV-vis spectrum of sensor **L1** in a CH_3CN/H_2O solution (9 : 1, v/v, 10 mM HEPES buffer, pH 7.4) exhibited one strong band at 290 nm which may be attributed to the π–π* transitions of the terpyridine unit.[22]

With gradual addition of Zn^{2+} to the solution of **L1**, the absorbance at 290 nm gradually decreased with concomitant formation of a new peak at 327 nm and an isosbestic point at 312 nm was observed (Fig. 1). The peaks at 312 nm and 327 nm might be attributed to the formation of a terpyridine bound zinc complex in sensor **L1**. By contrast, no significant absorption spectral change was observed for other cations such as Li^+, K^+, Na^+, Mg^{2+}, Ca^{2+}, Sr^{2+}, Ba^{2+}, Mn^{2+}, Fe^{2+}, Co^{2+}, Ni^{2+}, Cu^{2+}, Cd^{2+}, Pb^{2+}, Hg^{2+}, Pd^{2+}, Al^{3+} and Ag^+, under similar experimental conditions (Fig. S6†).

The fluorescence emission spectrum from 336 to 500 nm was recorded by exciting sensor **L1** at 312 nm. As shown in Fig. 2a, the free sensor **L1** (quantum yield ϕ = 0.0005) (Table S4†) showed no fluorescence in the CH_3CN/H_2O solution (9 : 1, v/v, 10 mM HEPES buffer, pH 7.4) but on incremental addition of Zn^{2+}, the fluorescence intensity at 370 nm

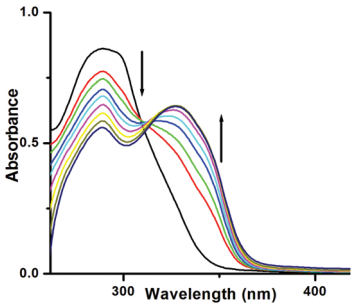

Fig. 1 Changes in UV-vis spectra of probe **L1** (4×10^{-5} M) upon gradual addition of Zn^{2+} ($c = 4 \times 10^{-4}$ M) in CH_3CN/H_2O solution (9 : 1, v/v, 10 mM HEPES buffer, pH 7.4).

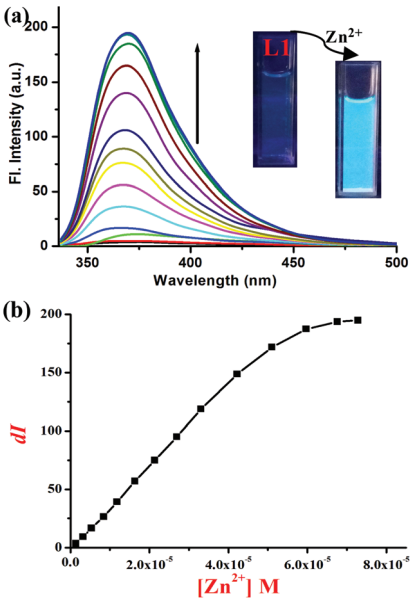

Fig. 2 (a) Fluorescence emission changes of **L1** (4×10^{-5} M) with the continuous addition of Zn^{2+} ($c = 4 \times 10^{-4}$ M) in CH_3CN/H_2O solution (9 : 1, v/v, 10 mM HEPES buffer, pH 7.4). λ_{ext} = 312 nm. Inset: Visual emission color changes of **L1** in the presence of Zn^{2+}. (b) Change of emission intensity at 370 nm with incremental addition of Zn^{2+} (λ_{ext} = 312 nm).

increased progressively and reached saturation with an ~51-fold enhancement (quantum yield $\phi = 0.0254$) (Table S4†) in integrated intensity. In the presence of Zn^{2+} ions, the fluorescence intensity of sensor **L1** increased in a Zn^{2+} concentration-dependent way as shown in Fig. 2b, accompanied by an apparent emission color change from colorless to sky blue. Hence, compound **L1** can be considered as being a real fluorescent off–on chemosensor. Such a fluorescence enhancement by Zn^{2+} might be due to the efficient coordination of Zn^{2+}, causing the chelation-enhanced fluorescence (CHEF) effect which is attributed to the energy minimization due to ligand to metal charge transfer.

From the fluorescence titration profile, the association constant of **L1** with the Zn^{2+} ion has been determined to be 1.85×10^4 ($R^2 = 0.993$), from the Benesi–Hildebrand equation.[20] The observed high K_a value clearly points out strong binding affinity of Zn^{2+} to probe **L1**. The detection limit[19] was evaluated to be 9.76 μM, which is below the Zn^{2+} concentration of the WHO guidelines for drinking water,[23] suggesting that **L1** is potentially useful for quantitative determination of Zn^{2+} in the environment and also for monitoring zinc ions in living cells.

Moreover, a careful Job plot analysis using fluorescence titration experiment suggested a 1 : 2 binding stoichiometry between **L1** and Zn^{2+} (Fig. S9†). In addition, the formation of a 1 : 2 complex (receptor : metal) was further confirmed through mass spectral analysis of the **L1**–Zn^{2+} complex, in which the peak at m/z 243.0867, assignable to [**L1** + $2Zn^{2+}$ + OH^- + CH_3CN]$^{3+}$, was clearly observed (Fig. S3†).

An imperative feature of probe **L1** is its high selectivity toward the zinc ion over the other competitive metal ions. As shown in Fig. 3, the initial fluorescence intensity of probe **L1** did not change significantly upon addition of 10 equivalents of different comparative metal cations such as Li^+, K^+, Na^+, Mg^{2+}, Ca^{2+}, Sr^{2+}, Ba^{2+}, Mn^{2+}, Fe^{2+}, Co^{2+}, Ni^{2+}, Cu^{2+}, Cd^{2+}, Pb^{2+}, Hg^{2+}, Pd^{2+}, Al^{3+} and Ag^+ to the semi-aqueous solution of **L1**, but in the presence of zinc ions **L1** showed a large fluorescence intensity enhancement at 370 nm. Only in the presence of Zn^{2+}, sensor **L1** showed a visual emission color change from non-fluorescent to sky blue during the above process. Thus, the probe **L1** can be used as a highly selective and specific chemosensor for zinc ions over other competing metal ions in several environmental and biological systems. Such high selectivity of **L1** for Zn^{2+} is mainly due to the high affinity of Zn^{2+} for three nitrogen atoms of the terpyridine moieties (Scheme 2).

Similar fluorescence studies were carried out in the presence of Zn^{2+} with the other two control molecules **L2** and **L3** (Fig. S13 & S14†) and found very small changes in fluorescence intensity (only ~4 fold for **L2** and only ~7 fold for **L3**) in the emission compared to **L1** (~51-fold), suggesting a sensitive detection of Zn^{2+} only by **L1** compared to the other two control molecules.

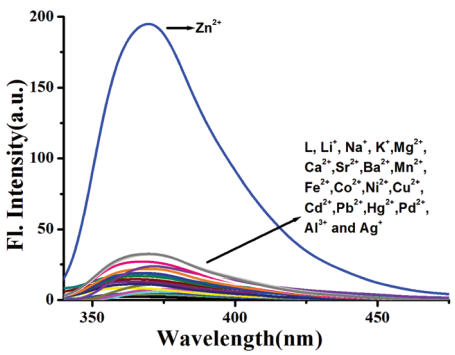

Fig. 3 Fluorescence response of **L1** to different competitive metal ions in CH_3CN/H_2O solution (9 : 1, v/v, 10 mM HEPES buffer, pH 7.4).

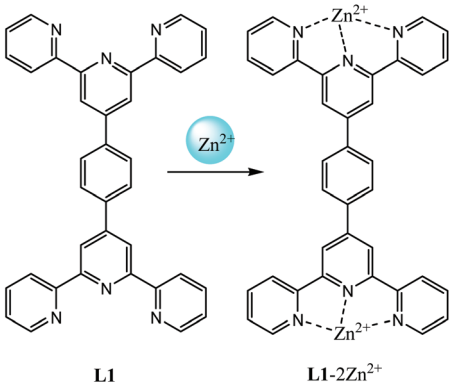

Scheme 2 Probable binding modes of **L1** and Zn^{2+} in the solution phase.

Theoretical study

To gain insight into the geometry of probe **L1** and **L1**–Zn^{2+} and the optical response of **L1** towards Zn^{2+}, we performed density functional theory (DFT) and time-dependent density functional theory (TD-DFT) calculations with the B3LYP/6-311+G(d,p) basis set using the Gaussian 09 program.[18] The optimized geometries along with the highest occupied molecular orbital (HOMO) and the lowest unoccupied molecular orbital (LUMO) of **L1** and **L1**–$2Zn^{2+}$ complex are presented in Fig. 4. From these HOMO and LUMO energy diagrams, we found that the energy gap for the **L1**–$2Zn^{2+}$ complex (90.90 kcal mol^{-1}) was reduced compared to that of probe **L1** alone (108.80 kcal mol^{-1}) (Table S1†), indicating that probe **L1** formed a stable di-nuclear zinc complex as shown in Fig. 5. The initial peak at 290 nm of **L1** in the absorbance spectra is due to the HOMO–LUMO transition. In the case of the Zn-complex, a bathochromic shift (312 nm) in the absorbance spectra was observed due to minimization of energy, owing to ligand to metal charge transfer. As shown in Fig. 5, the π-electron cloud in the HOMO is mainly located at the center of the **L1**–$2Zn^{2+}$ complex, which is spread out to all over the molecule in the LUMO, indicating that the LMCT phenomenon leads to the bathochromic shift and enhancement in fluorescence intensity.

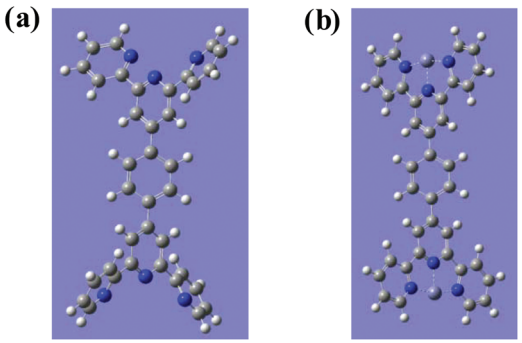

Fig. 4 Calculated energy-minimized structures of (a) **L1** and (b) **L1**–$2Zn^{2+}$ complex.

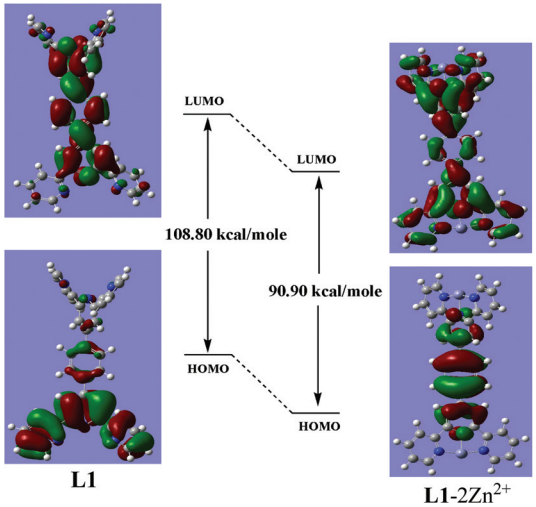

Fig. 5 HOMO and LUMO distributions of **L1** and **L1**–$2Zn^{2+}$ complex.

TD-DFT calculations have been carried out by the TD-DFT/CPCM method in acetonitrile solvent. Calculated wavelengths and oscillator frequencies from the TD-DFT calculations are listed in Table S2 (ESI†) and from these data we found that the calculated vertical electronic excitation matched well with the experimentally observed bands for both the **L1** probe and **L1**–$2Zn^{2+}$ complex.

Cell imaging study

In order to demonstrate the prospective biological application of sensor **L1**, fluorescence based bio-imaging experiments were carried out using MDA-MB-468 cells. However, to achieve this goal, it was essential to initially assess the cytotoxic effect of probe **L1** on live cells. The well-established MTT (3-(4,5-dimethylthiazol-2-yl)-2,5-diphenyltetrazolium bromide) assay, which is based on the mitochondrial dehydrogenase activity of viable cells, showed that neither **L1** nor its zinc complex were capable of revealing any effect on the viability of MDA-MB-468 cells (Fig. S11 & S12†). The results obtained from the *in vitro* cytotoxic assay suggested that probe concentrations up to 40 μM can be employed for the fluorescence imaging studies of **L1** and **L1**–$2Zn^{2+}$ in living cells. Hence, to assess the efficacy of probe **L1** as a chemosensor for intracellular detection of Zn^{2+} by confocal microscopy, MDA-MB-468 cells were treated with 20 μM $ZnCl_2$ for 1 h followed by incubation with 10 μM probe solution to encourage the formation of **L1**–$2Zn^{2+}$. From this fluorescence microscopy study, it was found that either probe **L1** or $ZnCl_2$ alone failed to display any fluorescence in MDA-MB-468 cells. However, upon incubation with $ZnCl_2$ followed by probe **L1**, distinctive turn-on blue fluorescence was observed inside the cells, which could be attributed to the formation of the intracellular di-nuclear zinc complex, as observed earlier in solution studies. Moreover, bright-field images of cells did not demonstrate any gross morphological changes, signifying that the MDA-MB-468 cells were viable throughout the bio-imaging experiments. These results indi-

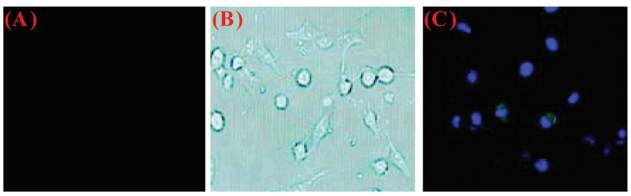

Fig. 6 Confocal microscopic image of **L1**-treated MDA-MB-468 cells before (A) and after (B &C) incubation with $ZnCl_2$. (A & C) represent the dark field image and (B) represents the bright-field image.

cate that probe **L1** is cell membrane permeable and can be employed for sensing intracellular zinc ions in living cells (Fig. 6).

Conclusions

In conclusion, we have designed and synthesized a highly selective and sensitive terpyridine based fluorescent "turn-on" chemosensor **L1** for Zn^{2+} ions among the other biologically important eighteen different metal ions studied in CH_3CN/H_2O solution (9 : 1, v/v, 10 mM HEPES buffer, pH 7.4). We have simultaneously studied the fluorescence sensing behaviour of two other terpyridine based chemosensors (**L2** and **L3**) towards Zn^{2+} but they are not so effective. Unlike most of the fluorescent probes, our reported chemosensor **L1** can be synthesized in a single step using low cost and commercially available starting materials with satisfactory yield. The entire reaction can be carried out in one pot and at room temperature. It can selectively detect Zn^{2+} ion down to 9.76 μM which is below the WHO guidelines for drinking water (76 μM) and the whole process is economically favorable. The sensor **L1** shows an obvious fluorescence enhancement (~51-fold) upon complexation with Zn^{2+} in semi-aqueous solution with a fluorescence color change from dark to sky blue. The selectivity and sensitivity of **L1** was demonstrated on the basis of fluorescence, absorption, and ESI mass spectrometry data. The association constant for **L1** with Zn^{2+} is in the order of 10^4 M^{-1} based on fluorescence spectral studies, signifying a strong binding for Zn^{2+}. Moreover, the Zn^{2+} binding nature of **L1** has been studied by computational calculations at the DFT level and TD-DFT calculations were also performed to show the electronic properties of **L1** and their corresponding zinc complexes. From these theoretical studies, we have found noteworthy similarities with the experimental results. Furthermore, the cell imaging experiments showed that **L1** was cell permeable and shows large fluorescence enhancement at pH 7.4. Thus, it can be applied for imaging and monitoring zinc ions in living cells.

Conflicts of interest

There is no conflict to declare.

Acknowledgements

TM and AH thankfully acknowledge the UGC, New Delhi for senior research fellowships. SP and SKM thank Haldia Government College for laboratory facility. AD is grateful to UGC, India for the DSK Postdoctoral fellowship.

References

1 (*a*) R. P. Haugland, *The handbook: a guide to fluorescent probes and labeling technologies*, Molecular Probes, 2005; (*b*) J. E. Kwon, S. Lee, Y. You, K. H. Baek, K. Ohkubo, J. Cho, S. Fukuzumi, I. Shin, S. Y. Park and W. Nam, *Inorg. Chem.*, 2012, **51**, 8760–8774; (*c*) B. Valeur and I. Leray, *Coord. Chem. Rev.*, 2000, **205**, 3–40; (*d*) P. G. Georgopoulos, A. Roy, M. J. Yonone-Lioy, R. E. Opiekun and P. J. Lioy, *J. Toxicol. Environ. Health, Part B*, 2001, **4**, 341–394; (*e*) R. Y. Tsien, *Fluorescent and photochemical probes of dynamic biochemical signals inside living Cell*, American Chemical Society, Washington, DC, USA, 1993, pp. 130–146.

2 (*a*) S. K. Kim, D. H. Lee, J. Hong and J. Yoon, *Acc. Chem. Res.*, 2009, **42**, 23–31; (*b*) J. Zhao, Y. Wang, W. Dong, Y. Wu, D. Li and Q. Zhang, *Inorg. Chem.*, 2016, **55**, 3265–3271.

3 (*a*) B. L. Vallee and K. H. Falchuk, *Physiol. Rev.*, 1993, **73**, 79–118; (*b*) S. C. Burdette and S. J. Lippard, *Proc. Natl. Acad. Sci. U. S. A.*, 2003, **100**, 3605–3610; (*c*) Z. K. Wu, Y. F. Zhang, J. S. Ma and G. Yang, *Inorg. Chem.*, 2006, **45**, 3140–3142; (*d*) A. S. Prasad, *Nutrition*, 1995, **11**, 93–99.

4 (*a*) J. M. Berg and Y. Shi, *Science*, 1996, **271**, 1081–1085; (*b*) W. N. Lipscomb and N. Sträter, *Chem. Rev.*, 1996, **96**, 2375–2433; (*c*) T. Kambe, Y. Yamaguchi-Iwai, R. Sasaki and M. Nagao, *Cell. Mol. Life Sci.*, 2004, **61**, 49–68; (*d*) P. Jiang and Z. Guo, *Coord. Chem. Rev.*, 2004, **248**, 205–229; (*e*) S. Yamasaki, K. Sakata-Sogawa, A. Hasegawa, T. Suzuki, K. Kabu, E. Sato, T. Kurosaki, S. Yamashita, M. Tokunaga, K. Nishida and T. Hirano, *J. Cell Biol.*, 2007, **177**, 637–645.

5 (*a*) J. J. R. F. da Silva and R. J. P. Williams, *The biological chemistry of the elements: the inorganic chemistry of life*, Oxford University Press, Oxford, 2001, pp. 315–335; (*b*) B. L. Vallee and D. S. Auld, *Acc. Chem. Res.*, 1993, **26**, 543–551; (*c*) A. I. Bush, W. H. Pettingell, G. Multhaup, M. D. Paradis, J. P. Vonsattel, J. F. Gusella, K. Beyreuther, C. L. Masters and R. E. Tanzi, *Science*, 1994, **265**, 1464–1468.

6 (*a*) C. J. Frederickson, S. W. Suh, D. Silva, C. J. Frederickson and R. B. Thompson, *J. Nutr.*, 2000, **130**, 1471S–1483S; (*b*) D. W. Choi and J. Y. Koh, *Annu. Rev. Neurosci.*, 1998, **21**, 347–375; (*c*) W. Maret, C. Jacob, B. L. Vallee and E. H. Fischer, *Proc. Natl. Acad. Sci. U. S. A.*, 1999, **96**, 1936–1940.

7 (*a*) P. J. Fraker and L. E. King, *Annu. Rev. Nutr.*, 2004, **24**, 277–298; (*b*) M. P. Cuajungco and G. J. Lees, *Neurobiol. Dis.*, 1997, **4**, 137–169; (*c*) S. Frassinetti, G. L. Bronzetti,

L. Caltavuturo, M. Cini and C. Della Croce, *J. Environ. Pathol., Toxicol. Oncol.*, 2006, **25**, 597–610.

8 (*a*) X. Chen, T. Pradhan, F. Wang, J. S. Kim and J. Yoon, *Chem. Rev.*, 2012, **112**, 1910–1956; (*b*) J. H. Weiss, S. L. Sensi and J. Y. Koh, *Trends Pharmacol. Sci.*, 2000, **21**, 395–401.

9 (*a*) A. I. Bush, *Alzheimer Dis. Assoc. Disord.*, 2003, **17**, 147–150; (*b*) C. J. Frederickson, M. D. Hernandez and J. F. McGinty, *Brain Res.*, 1989, **480**, 317–321; (*c*) K. S. Aboody, A. Brown, N. G. Rainov, K. A. Bower, S. Liu, W. Yang, J. E. Small, U. Herrlinger, V. Ourednik, P. M. Black and X. O. Breakefield, *Proc. Natl. Acad. Sci. U. S. A.*, 2000, **97**, 12846–12851.

10 (*a*) J. F. Zhang, S. Bhuniya, Y. H. Lee, C. Bae, J. H. Lee and J. S. Kim, *Tetrahedron Lett.*, 2010, **51**, 3719–3723; (*b*) A. Voegelin, S. Pfister, A. C. Scheinost, M. A. Marcus and R. Kretzschmar, *Environ. Sci. Technol.*, 2005, **39**, 6616–6623; (*c*) E. Callender and K. C. Rice, *Environ. Sci. Technol.*, 2000, **34**, 232–238; (*d*) L. Li, Y. Q. Dang, H. W. Li, B. Wang and Y. Wu, *Tetrahedron Lett.*, 2010, **51**, 618–621.

11 (*a*) Z. Xu, J. Yoon and D. R. Spring, *Chem. Soc. Rev.*, 2010, **39**, 1996–2006; (*b*) P. Carol, S. Sreejith and A. Ajayaghosh, *Chem. – Asian J.*, 2007, **2**, 338–348; (*c*) E. Kimura and T. Koike, *Chem. Soc. Rev.*, 1998, **27**, 179–184; (*d*) H. G. Lee, J. H. Lee, S. P. Jang, H. M. Park, S. Kim, Y. Kim, C. Kim and R. G. Harrison, *Tetrahedron*, 2011, **67**, 8073–8078.

12 (*a*) A. K. Mahapatra, S. K. Manna, C. D. Mukhopadhyay and D. Mandal, *Sens. Actuators, B*, 2014, **200**, 123–131; (*b*) S. A. Ingale and F. Seela, *J. Org. Chem.*, 2012, **77**, 9352–9356; (*c*) G. J. Park, M. M. Lee, G. R. You, Y. W. Choi and C. Kim, *Tetrahedron Lett.*, 2014, **55**, 2517–2522; (*d*) Y. Chen, Y. Bai, Z. Han, W. He and Z. Guo, *Chem. Soc. Rev.*, 2015, **44**, 4517–4546.

13 (*a*) J. Wang, Y. Li, E. Duah, S. Paruchuri, D. Zhou and Y. Pang, *J. Mater. Chem. B*, 2014, **2**, 2008–2012; (*b*) S. Lohar, S. Pal, M. Mukherjee, A. Maji, N. Demitri and P. Chattopadhyay, *RSC Adv.*, 2017, **7**, 25528–25534; (*c*) Z. Dai and J. W. Canary, *New J. Chem.*, 2007, **31**, 1708–1718; (*d*) M. Macias-Contreras, K. L. Daykin, J. T. Simmons, J. R. Allen, Z. S. Hooper, M. W. Davidson and L. Zhu, *Org. Biomol. Chem.*, 2017, **15**, 9139–9148.

14 (*a*) P. S. Yao, Z. Liu, J. Z. Ge, Y. Chen and Q. Y. Cao, *Dalton Trans.*, 2015, **44**, 7470–7476; (*b*) A. Gogoi, S. Samanta and G. Das, *Sens. Actuators, B*, 2014, **202**, 788–794.

15 (*a*) S. Goswami, A. K. Das, K. Aich, A. Manna, S. Maity, K. Khanra and N. Bhattacharyya, *Analyst*, 2013, **138**, 4593–4598; (*b*) Y. Ma, H. Chen, F. Wang, S. Kambam, Y. Wang, C. Mao and X. Chen, *Dyes Pigm.*, 2014, **102**, 301–307.

16 (*a*) P. Manna, S. K. Seth, M. Mitra, S. R. Choudhury, A. Bauzá, A. Frontera and S. Mukhopadhyay, *Cryst. Growth Des.*, 2014, **14**, 5812–5821; (*b*) A. Das, A. D. Jana, S. K. Seth, B. Dey, S. R. Choudhury, T. Kar, S. Mukhopadhyay, N. J. Singh, I. C. Hwang and K. S. Kim, *J. Phys. Chem. B*, 2010, **114**, 4166–4170; (*c*) P. Manna, S. K. Seth, A. Bauzá, M. Mitra, S. R. Choudhury, A. Frontera and S. Mukhopadhyay, *Cryst. Growth Des.*, 2014, **14**, 747–755; (*d*) H. Hofmeier and U. S. Schubert, *Chem. Soc. Rev.*, 2004, **33**, 373–399; (*e*) A. Wild, A. Winter, F. Schlütter and U. S. Schubert, *Chem. Soc. Rev.*, 2011, **40**, 1459–1511; (*f*) T. Yasuda, I. Yamaguchi and T. Yamamoto, *Adv. Mater.*, 2003, **15**, 293–296; (*g*) H. Li, S. J. Zhang, C. L. Gong, Y. F. Li, Y. Liang, Z. G. Qi and S. Chen, *Analyst*, 2013, **138**, 7090–7093; (*h*) B. G. Lohmeijer and U. S. Schubert, *Macromol. Chem. Phys.*, 2003, **204**, 1072–1078; (*i*) R. Dobrawa, M. Lysetska, P. Ballester, M. Grüne and F. Würthner, *Macromolecules*, 2005, **38**, 1315–1325.

17 (*a*) P. C. Yang, H. Wu, C. L. Lee, W. C. Chen, H. J. He and M. T. Chen, *Polymer*, 2013, **54**, 1080–1090; (*b*) X. Lou, Y. Zhang, S. Li, D. Ou, Z. Wan, J. Qin and Z. Li, *Polym. Chem.*, 2012, **3**, 1446–1452.

18 M. J. Frisch, G. W. Trucks, H. B. Schlegel, G. E. Scuseria, M. A. Robb, J. R. Cheeseman, G. Scalmani, V. Barone, B. Mennucci, G. A. Petersson, H. Nakatsuji, M. Caricato, X. Li, H. P. Hratchian, A. F. Izmaylov, J. Bloino, G. Zheng, J. L. Sonnenberg, M. Hada, M. Ehara, K. Toyota, R. Fukuda, J. Hasegawa, M. Ishida, T. Nakajima, Y. Honda, O. Kitao, H. Nakai, T. Vreven, J. A. Montgomery, J. J. E. Peralta, F. Ogliaro, M. Bearpark, J. J. Heyd, E. Brothers, K. N. Kudin, V. N. Staroverov, T. Keith, R. Kobayashi, J. Normand, K. Raghavachari, A. Rendell, J. C. Burant, S. S. Iyengar, J. Tomasi, M. Cossi, N. Rega, J. M. Millam, M. Klene, J. E. Knox, J. B. Cross, V. Bakken, C. Adamo, J. Jaramillo, R. Gomperts, R. E. Stratmann, O. Yazyev, A. J. Austin, R. Cammi, C. Pomelli, J. W. Ochterski, R. L. Martin, K. Morokuma, V. G. Zakrzewski, G. A. Voth, P. Salvador, J. J. Dannenberg, S. Dapprich, A. D. Daniels, O. Farkas, J. B. Foresman, J. V. Ortiz, J. Cioslowski and D. J. Fox, *Gaussian 09, Revision D.01*, Gaussian, Wallingford, CT, 2013.

19 (*a*) L. Long, D. Zhang, X. Li, J. Zhang, C. Zhang and L. Zhou, *Anal. Chim. Acta*, 2013, **775**, 100–105; (*b*) S. Mondal, S. K. Manna, K. Maiti, R. Maji, S. S. Ali, S. Manna, S. Mandal, M. R. Uddin and A. K. Mahapatra, *Supramol. Chem.*, 2017, **29**, 616–626; (*c*) S. Goswami, A. Manna, S. Paul, K. Aich, A. K. Das and S. Chakraborty, *Dalton Trans.*, 2013, **42**, 8078–8085.

20 (*a*) H. A. Benesi and J. H. Hildebrand, *J. Am. Chem. Soc.*, 1949, **71**, 2703–2707; (*b*) Y. Shiraishi, S. Sumiya, Y. Kohno and T. Hirai, *J. Org. Chem.*, 2008, **73**, 8571–8574; (*c*) C. Yang, L. Liu, T. W. Mu and Q. X. GUO, *Anal. Sci.*, 2000, **16**, 537–539.

21 A. Duerrbeck, S. Gorelik, J. Hobley, A. M. Yong, G. S. Subramanian, A. Hor and N. Long, *J. Mater. Chem. C*, 2015, **3**, 8992–9002.

22 A. D'Aléo, E. Cecchetto, L. De Cola and R. M. Williams, *Sensors*, 2009, **9**, 3604–3626.

23 (*a*) Y. P. Kumar, P. King and V. S. R. K. Prasad, *Chem. Eng. J.*, 2006, **124**, 63–70; (*b*) J. H. Kim, J. Y. Noh, I. H. Hwang, J. Kang, J. Kim and C. Kim, *Tetrahedron Lett.*, 2013, **56**, 2415–2418.

